23rd ABCM International Congress of Mechanical Engineering
December 6-11, 2015, Rio de Janeiro, RJ, Brazil

A NUMERICAL STUDY OF LOCALIZED PULSED ENERGY DEPOSITION IN STAGNANT AIR AND HIGH SPEED AIRFLOWS

André Carlos Fraile Júnior
Mauricio Antoniazzi Pinheiro Rosa
Instituto de Estudos Avançados – Divisão de Aerotermodinâmica e Hipersônica, Trevo Coronel Aviador José Alberto Albano do Amarante, 1, CEP 12.228-001, São José dos Campos/SP, Brazil.
fraile@ieav.cta.br , pinheiro@ieav.cta.br

Abstract. *Energy deposition to high speed airflows is widely studied in applications such as wave drag reduction, optimization of scramjet inlets, sonic boom mitigation, ignition of a combustible gas mixture and so on. This work presents a numerical analysis of pulsed energy deposition as a localized heat source in stagnant air and in uniform supersonic airflows. Firstly, it was performed a detailed study concerning the choice of numerical methods in the Fluent code and mesh sizing. Next, it was performed a parametric analysis, for single and multiple pulse heat sources, of the effects of energy deposition on the flow properties when pulse duration, energy deposition rate and pulse frequency are varied. Results have shown that increasing the energy deposition rate or the pulse duration has the effect of pronouncing flow changes such as the temperature increase and density decrease along the source axis.*

Keywords: *flow control, energy addition, supersonic flow.*

1. INTRODUCTION

A major design goal for supersonic vehicles is to operate at very high speeds without generating excessive drag (Riggins and Nelson, 1999). Several techniques have been proposed to reduce this wave drag in such vehicles like, for example, using physical structures at the nose of the vehicle, which modify the shock wave geometry. However, this method also generates excessive stress at this additional structure (Riggins *et al.*, 1999; Riggins and Nelson, 1999; Knight, 2003). Other methods employed in order to reduce wave drag consist of the addition of gas flow opposed to the free stream (Yisheng, 2013) and also the use of porous materials (Formin *et al.*, 2009). Recent studies have been made in order to overcome some of the difficulties imposed by these methods of drag reduction concerning the energy addition to airflows upstream to the vehicles. Besides the improvements to wave drag, energy addition may also be employed to modify scramjet performance (inlet mass capture and isolator shortening) and to control attitude of high speed vehicles (Riggins *et al.* 1999; Riggins and Nelson, 1999; Knight, 2003).

In the Institute for Advanced Studies (IEAv) previous experimental works about energy addition by laser pulses were conducted (Oliveira, 2008a; Oliveira, 2008b; Oliveira, 2008c; Salvador, 2005; Salvador, 2007; Salvador, 2008) and motivated numerical studies that considered the problem of energy addition to high speed airflows with blunt bodies in order to reduce wave drag (Fraile Jr., 2011; Fraile Jr. and Rosa, 2013). However, in order to study the effects of employing energy addition to reduce wave drag, it is necessary to understand how localized energy deposition affects high speed airflow properties. With this in mind, this work has the objective of studying numerically how stagnant air and supersonic airflows are affected by single pulse and multiple pulse localized energy depositions in a spherical region of the flow. Here, the energy source is treated by thermodynamics and gas dynamics standpoints, so it only transfers thermal energy to the air. The results have shown that increasing the energy deposition rate or the pulse duration has the effect of pronouncing flow changes such as the temperature increase and the density decrease along the flow direction downstream to the source. The studies developed in this work concerning the effects of energy addition to high speed airflows will be used in future works to further understand the phenomena involved in hypersonic applications such as blunt body wave drag reduction and improvement of scramjet performance.

2. METHODOLOGY

In this work, the Navier-Stokes equations for inviscid flow have been used in order to study the airflow (FLUENT Inc., 2006):

$$\begin{cases} \dfrac{\partial \rho}{\partial t} + \nabla \cdot \left(\rho \vec{v} \right) = 0 \\ \dfrac{\partial}{\partial t}\left(\rho \vec{v} \right) + \nabla \cdot \left(\rho \vec{v}\vec{v} \right) = -\nabla p \\ \dfrac{\partial}{\partial t}\left(\rho E \right) + \nabla \cdot \left[\left(\rho E + p \right) \vec{v} \right] = k\nabla^2 T + Q \end{cases} \tag{1}$$

where t is the time, ρ is the flow density, p is the static pressure, $\vec{v}$ is the velocity vector, k is the thermal conductivity, E is the total energy per mass unit, T is the static temperature and Q is the energy source term.

Since the gas is considered ideal in this work, it is possible to express the pressure as a function of density, temperature and gas constant (R):

$$p = \rho R T \tag{2}$$

The energy per mass unit may also be written as a function of flow variables:

$$E = h - \frac{p}{\rho} + \frac{v^2}{2} \tag{3}$$

where $dh = c_p dT$.

The source term in Eq. (1) expresses the energy rate per unit volume and may be defined as (Georgievskii *et al.*, 2006):

$$Q\left(x, y, t \right) = \rho Q_0 \exp\left(-\frac{x^2}{d_x^2} - \frac{y^2}{d_y^2} \right) \phi_p\left(t \right) \tag{4}$$

where d_x and d_y are parameters that define the energy source dispersion and Q_0 is a constant related to the magnitude of the energy rate deposition.

This constant may be normalized by the following relation (Georgievskii *et al.*, 2006):

$$\bar{Q}_0 = Q_0 \frac{\left(p_\infty / \rho_\infty \right)^{3/2}}{l} \tag{5}$$

where l = 1 cm is the characteristic length. The free stream pressure and density are presented here as p_∞ and ρ_∞.

The function $\phi_p(t)$ defines the temporal dependency of the energy source term. For a steady energy source, $\phi_p(t) = 1$ for any t. If, however, energy is being deposited as a single pulse of duration τ_p time units, then:

$$\phi_p\left(t \right) = \begin{cases} 1, \text{ if } t \le \tau_p \\ 0, \text{ if } t > \tau_p \end{cases} \tag{6}$$

The pulse duration τ_p may also be normalized by the following equation (Georgievskii *et al.*, 2006):

$$\bar{\tau}_p = \frac{\tau_p}{l} \sqrt{\frac{p_\infty}{\rho_\infty}} \tag{7}$$

For multiple pulses deposition, the function $\phi_p(t)$ may be defined as:

$$\phi_p\left(t \right) = \begin{cases} 1, \text{ if } \operatorname{mod}\left(t, T_p \right) \le \tau_p \\ 0, \text{ if } \operatorname{mod}\left(t, T_p \right) > \tau_p \end{cases} \tag{8}$$

where T_p is the period of pulses deposition and mod(t, T_p) is the module function.

These equations are solved using the density-based approach available in the FLUENT® solver for the axisymmetric geometry schematized in Fig. 1 (FLUENT Inc., 2006). The energy source center is located at the origin where the energy deposition peak takes place (see Eq. (4)).The conditions for the free stream supersonic flow are defined as $p_\infty = 1.29\times10^4$ Pa, T_∞ = 166 K and M_∞ = 4.0 (Mach number). When the fluid is initially stagnant, it is defined $M_\infty = 0$.

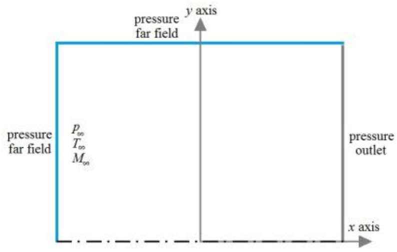

Figure 1. Physical domain used for calculations and boundary conditions applied to the solver

The fluid moves from the left to the right boundary of the physical domain, which has dimensions of 40 cm (horizontal) per 30 cm (vertical). As shown in Fig. 1, the left and upper boundaries of the domain are defined as pressure far field boundary conditions. The lower boundary is defined as symmetry axis while the right boundary is defined as pressure outlet. Energy addition to the airflow has been achieved by a user-defined function (UDF), which is a resource of the Fluent® *software* capable of modifying several parameters used while calculations are performed.

A square-element grid with 20 divisions per millimeter has been used to conduct the calculations in this work. The time step used in the transient method was set at 50 ns. In order to study the solution accuracy level, the spatial mesh was refined and the time step was reduced until differences between these results and those with larger elements and time step were negligible for the analyses performed.

3. NUMERICAL COMPARISON

In order to verify accuracy of the solutions obtained with the methodology employed in this work, some results presented by Geogievskii *et al*. (2006) were reproduced here. Figure 2 shows, for a steady energy source, the results shown in Fig. 3 of Geogievskii *et al*. (2006) and the same results obtained through the numerical method employed in this work. These results are related to the pressure and temperature distribution along the symmetry axis of a steady energy source with $\bar{Q}_0 = 100$ and $d_x = d_y = 0.15$ cm .

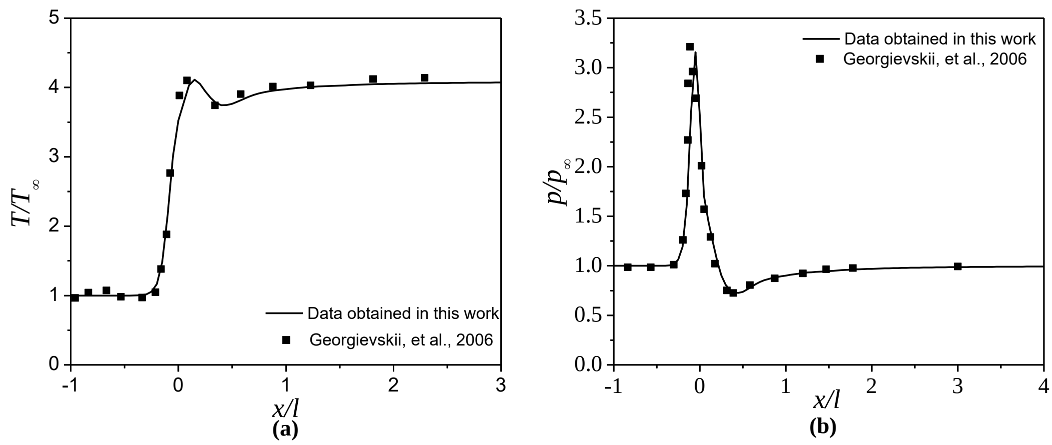

Figure 2. Comparison of flow properties along the symmetry axis between numerical method discussed in this work and the one by Georgievskii *et al.* (2006) for $\bar{Q}_0 = 100$ and $d_x = d_y = 0.15$ cm : (a) temperature; (b) pressure.

Figure 3 shows how the temperature is modified as a function of time (normalized by 45.7 μs) for several values of pulse duration at a point located downstream to the energy source center. These results may be compared to the ones available in Fig. 7 of Geogievskii *et al*. (2006), which presents the temperature distribution at a point location of the wake as a function of time. As can be seen, both methodologies presented quite similar results.

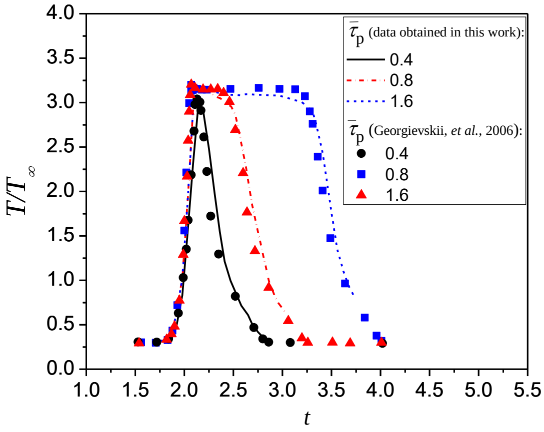

Figure 3. Comparison of temperature as a function of time (normalized by 45.7 μs) for a point downstream to the energy source with $\bar{Q}_0$ = 125, $d_x = 0.1$ cm and $d_y = 0.4$ cm .

4. RESULTS

The following section shows some results of a series of studies concerning the effects of pulsed energy addition to stagnant air and supersonic airflow.

4.1 Single-pulse energy deposition in stagnant air

In order to understand the overall effects of energy addition to an initially stagnant fluid, Fig. 4 shows the pressure and temperature fields associated to a single pulse deposition with $\bar{Q}_0$ = 300, τ_p = 4.57 μs (or $\bar{\tau}_p = 0.1$) at the time instant t = 75 μs. The source parameters are d_x = d_y = 0.5 cm. Figure 5 shows flow variables along the symmetry axis for two different conditions: $\bar{Q}_0$ = 100 and $\bar{Q}_0$ = 300 at time t = 75 μs.

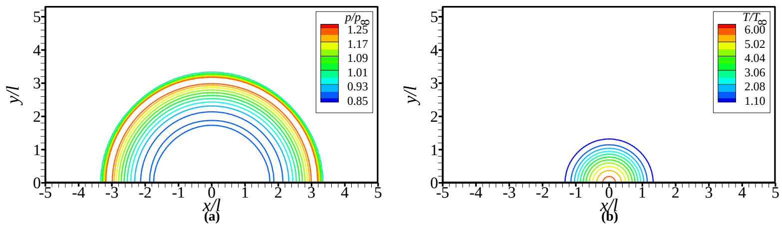

Figure 4. Scalar fields for stagnant air with energy addition: $\bar{Q}_0$ = 300, t = 75 μs: (a) pressure; (b) temperature.

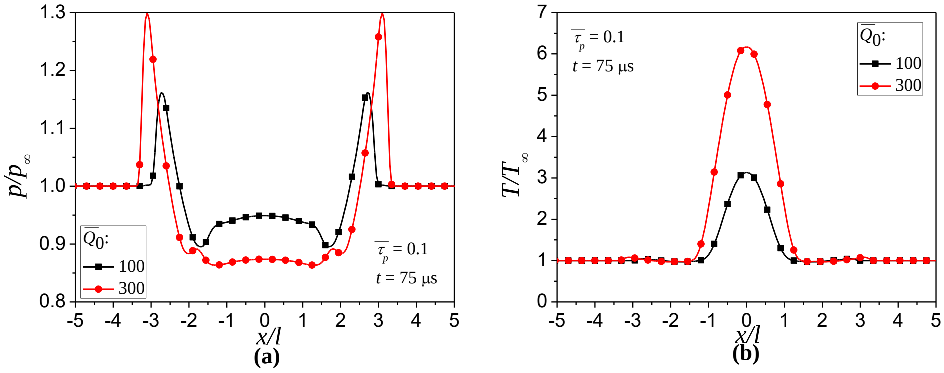

Figure 5. Flow properties on the symmetry axis for stagnant air at t = 75 μs: (a) pressure; (b) temperature.

As can be seen in Fig. 4 and 5, a spherical compression wave expands from the source center while the temperature rise takes place basically inside the energy addition region. The pressure increase near the wave front results in air flowing from the energy source center to the domain boundaries. The temperature increases near the energy source center and the density is actually decreased near this region since the pressure is reduced. It is also possible to verify from the pressure peaks positions in Fig. 5 that the wave front expands faster for the case with higher energy rate, which may be related to the higher temperature near the source region and, consequently, a higher sound velocity and also faster propagation of perturbations from the energy source.

4.2 Single-pulse energy deposition in supersonic airflows

Figure 6 shows the effects of energy addition to supersonic airflow on pressure and temperature contours for a free stream from the left to the right at Mach number $M_\infty = 4.0$. The energy source parameters are $\bar{Q}_0 = 300$, $\bar{\tau}_p = 0.5$, $d_x = d_y = 0.5$ cm.

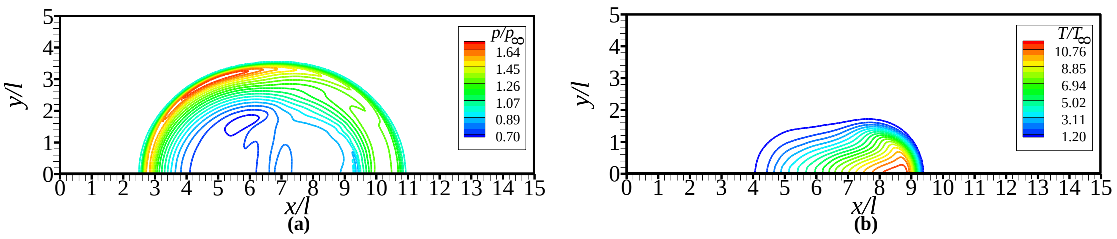

Figure 6. Pressure and temperature fields for supersonic flow with energy addition: $\bar{Q}_0$ = 300, t = 75 μs.

Figure 6(a) shows that the energy source generates a compression wave that travels downstream from its center. Comparing these results with the ones in Fig. 4 for stagnant air, it is possible to observe that the pressure also increases in the wave front, while a low pressure core is formed. However, when energy is deposited in supersonic flow, the spherical symmetry previously observed for stagnant air is not maintained anymore. It shows, however, a greater pressure increase along the left side of the wave portion located near the energy center since the flow is supersonic, which further increases the compression ratio there, as can be seen in Fig. 6(a). On the other hand, the temperature is increased near the energy source center and this region with temperature rise travels downstream to the energy source.

Figure 7 presents the effects of energy rate on the flow properties for $M_\infty = 4.0$, $\bar{\tau}_p = 0.5$ at t = 75 μs along the symmetry axis. This figure shows that higher values of the parameter $\bar{Q}_0$ have the effect of modifying the magnitude of flow properties. As previously observed for stagnant air, the position of the compression wave in Fig. 7(a) also indicates that higher energy rates increase the wave velocity for supersonic flows, which is associated to an increase in temperature.

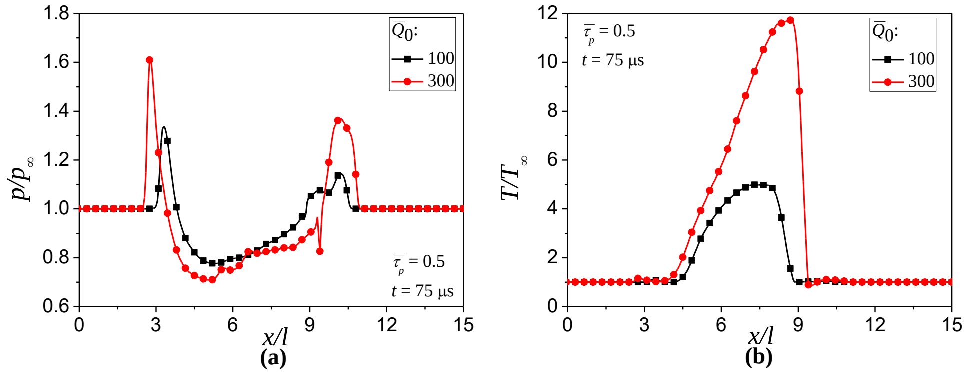

Figure 7. Supersonic flow properties with energy addition at t = 75 μs: (a) pressure; (b) temperature.

Figure 8 shows the effect of modifying the pulse duration for $\bar{Q}_0 = 300$ at the time instant 75 μs along the symmetry axis.The results presented in this figure show that increasing the energy deposition duration, the temperature of the region affected by energy addition is increased, while the pressure is maintained at a level lower than the free stream value. Although the minimum pressure achieved by both pulse durations shown in Fig. 8(a) is approximately the same, the airflow is kept longer at these modified conditions of higher temperature and lower density for a higher pulse duration.

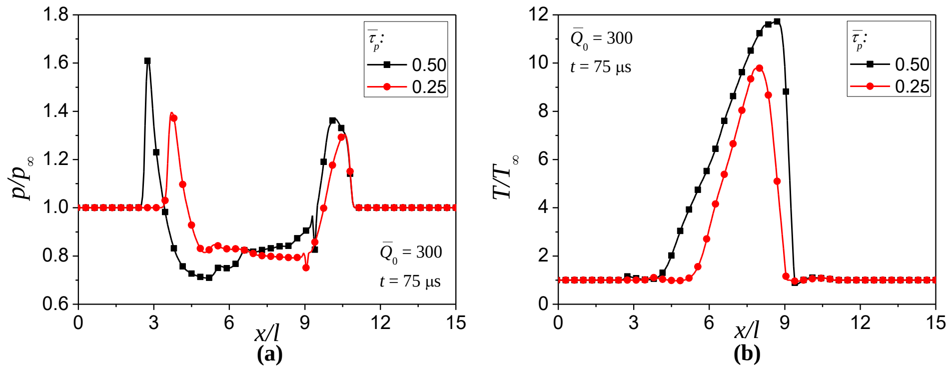

Figure 8. Effect of deposition duration for $\bar{Q}_0$ = 300 at t = 75 μs: (a) pressure; (b) temperature.

4.3 Multiple pulse energy deposition in supersonic airflows

This section presents the overall effects of multiple pulse energy addition to supersonic airflow. Figures 9 and 10 show pressure and temperature fields at t = 75 μs for cases with different period of pulses, T_p, while keeping the pulse duration, τ_p, the same ($\bar{\tau}_p = 0.1$), such that the ratio, T_p/τ_p ,is equal to 8 and 2, respectively, for $\bar{Q}_0$ = 300.

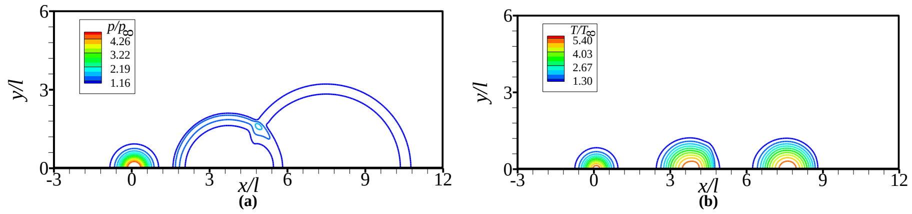

Figure 9. Scalar fields for $\bar{Q}_0$ = 300 and T_p/τ_p = 8 at t = 75 μs: (a) pressure; (b) temperature.

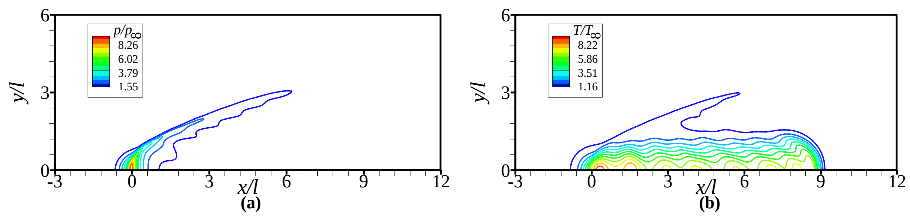

Figure 10. Scalar fields for $\bar{Q}_0$ = 300 and T_p/τ_p = 2 at t = 75 μs: (a) pressure; (b) temperature.

In Fig. 9, it can be seen a sequence of clearly separated waves produced by the energy pulses whereas in Fig. 10, due to the higher pulse frequency, the interaction between waves is more accentuated approaching that for steady energy deposition ($\tau_p = T_p$), i.e., the pressure increases near the energy source and then decreases donwstream to values closer to the free stream one along the symmetry axis, while the temperature is characterized by a stream tube of about the deposition region radius around the symmetry axis with higher values than the free stream one (Fraile Jr. and Rosa, 2013).

Figure 11 shows pressure and temperature distributions along the symmetry axis for the same conditions shown in Fig. 9 and 10.

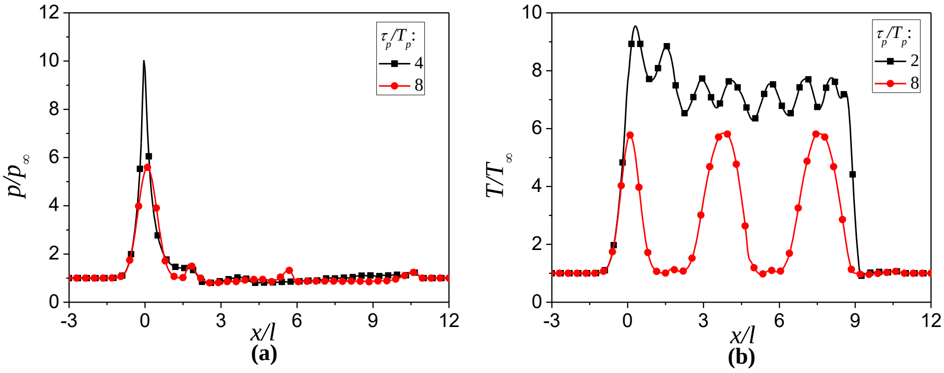

Figure 11. Flow variables along the symmetry axis for $\bar{Q}_0$ = 300 and different values of T_p/τ_p: (a) pressure; (b) temperature.

Since the source center is located at $x/l = 0$, all cases presented in Fig. 11 have shown pressure and temperature rise at this position. It is important to mention that, in this figure, the flow variables vanish for distances beyond $x/l = 9$ approximately, only because, at the time $t = 75$ μs, the flow there has not been affected by the energy deposition yet. Figure 11(b) shows that the ratio T_p/τ_p modifies the amplitude and the frequency of temperature variation in the region affected by the energy deposition. When T_p/τ_p is reduced, the frequency increases and the flow property changes are also reduced, since the pulse duration is kept the same, yielding higher temperature values along the symmetry axis. In the case where this ratio is further reduced, the temperature distribution along the symmetry axis becomes approximately uniform downstream to the energy source similarly to a steady energy deposition case (Fraile Jr. and Rosa, 2013).

Figure 12 shows the effect of changing both the pulse duration and the period of pulses, such that $T_p/\tau_p = 4$, on the flow properties along the symmetry axis at the instant of 75 μs with $\bar{Q}_0$ = 300.

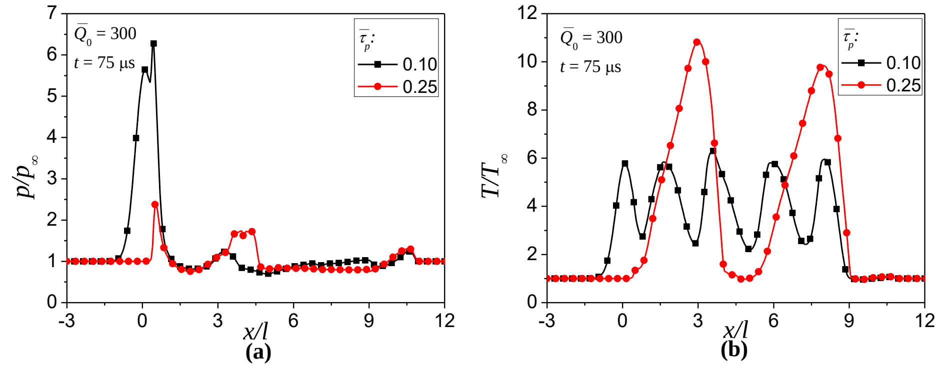

Figure 12. Flow variables along the symmetry axis for $\bar{Q}_0$ = 300 and $T_p/\tau_p = 4$ at instant 75 μs for different values of deposition pulse duration: (a) pressure; (b) temperature.

Figure 12 shows that, for constant ratio T_p/τ_p, as $\bar{\tau}_p$ is increased from 0.10 to 0.25, it yields higher temperature changes along the symmetry axis, although the number of pulses at the same time interval is smaller. It is worth mentioning that, while the temperature reaches higher values when $\bar{\tau}_p$ is increased, the pressure reaches lower values because there are less interactions between wave fronts of different energy pulses.

5. CONCLUSIONS

It has been presented some results of an analysis of the effects of localized pulsed energy addition to both stagnant fluid and to uniform supersonic airflows by changing parameters such as: energy deposition rate, pulse duration and frequency. For stagnant air, it was possible to verify that a spherical compression wave front propagates outwards from the center of the energy source. The magnitude of flow variables such as pressure, temperature and density is proportional to the energy rate added to the airflow. On the other hand, when the same form of pulsed energy is deposited on a supersonic airflow, the compression wave loses spherical symmetry and acquires an elongated axial symmetry, with the pressure increasing greatly at the region of the compression wave near the energy source. Results have shown that increasing the energy deposition rate or the pulse duration has the effect of pronouncing flow changes such as the temperature increase and density decrease along the source axis. When several pulses are deposited on the airflow, results have shown that flow variables are closer to the ones for steady energy addition if the ratio of pulse duration per period of deposition is closer to one, which is the limit of continuous energy deposition.

Results obtained with the numerical methodology employed in this work have compared well with the ones by Georgievskii *et al.*, 2006, which reinforces the adequacy of such a methodology. As any application of energy addition to high speed flow control requires a great knowledge of how the energy deposition, pulsed or steady, affects downstream flow properties, the analysis presented here will be very helpful for the ongoing numerical study, at the Institute for Advanced Studies (IEAv), of blunt body wave drag reduction by pulsed energy addition.

6. REFERENCES

FLUENT Inc., 2006. “FLUENT 6.3 User’s Guide”. 3 May 2013 <https://www.sharcnet.ca/Software/Fluent6/html/ug/main_pre.htm>.

Fomin, V. M. et al, 2009, “Reducing the wave drag of bodies in supersonic flows using porous materials”, Technical Physics Letters, Vol. 35, No. 2, pp. 117-119.

Fraile Jr., A. C. 2011, “Um estudo numérico da redução de arrasto em corpos rombudos por adição de energia em escoamentos de altas velocidades” (In Portuguese), Thesis, Instituto Tecnológico de Aeronáutica, 128 p.

Fraile Jr., A. C., Rosa, M. A. P., 2013, “A numerical investigation of localized and steady energy addition to high speed airflows”. J. Aerosp. Technol. Manag., Vol. 5, No. 2, pp. 169-180.

Georgievskii, P. Yu. And Levin, V. A., 2003. “Control of the flow past bodies using localized energy addition to the supersonic oncoming flow”. *Fluid Dynamics*, Vol. 38, p. 794.

Georgievskii, P. Yu., et al, 2006. “Transverse electric discharges in supersonic air flows: simulation of gasdynamic effects in the discharge channel”. *High Temperature*, Vol. 44, p. 001.

Knight, D., 2003, “Survey of Aerodynamic Flow Control at High Speed by Energy Deposition”. 41st AIAA Aerospace Sciences Meeting and Exhibit, 19 p.

Oliveira, A. C. et al, 2008a, “Bow shock wave mitigation by laser-plasma energy addition in hypersonic flow”, Journal of Spacecraft and Rockets, Vol. 45, No. 5, pp. 921-927.

Oliveira, A. C. et al, 2008b, “Drag Reduction by Laser-Plasma Energy Addition in Hypersonic Flow”, Fifth International Symposium on Beamed Energy Propulsion, Vol. 997, pp. 379-389.

Oliveira, A. C., 2008c, “Investigação experimental da adição de energia por laser em escoamento hipersônico de baixa densidade” (In Portuguese), Thesis, Instituto Nacional de Pesquisas Espaciais, 202 p.

Riggins, D. W. *et al.*, 1999, “Blunt-body wave drag reduction using focused energy deposition”, AIAA Journal, Vol. 37, No. 4, pp. 460-467.

Riggins, D. W., Nelson, H. F., 1999, “Hypersonic flow control using upstream focused energy deposition”, Aerospace Sciences Meeting & Exhibit, 37, Reno.

Salvador, I. I. et al, 2005, “Experimental Analysis of Heat Flux to a Blunt Body in Hypersonic Flow with Upstream Laser Energy Deposition - Preliminary Results”. 4th International Symposium on Beamed Energy Propulsion, Vol. 830, pp. 163-171.

Salvador, I. I. et al, 2008, “Experimental Analysis of Heat Flux to a Blunt Body in Hypersonic Flow with Upstream Laser Energy Deposition”, Fifth International Symposium on Beamed Energy Propulsion, Vol. 997, pp. 379-389.

Salvador, I. I. et al, 2007, “Surface Heat Flux and Pressure Distribution on a Hypersonic Blunt Body with DEAS”, Fifth International Symposium on Beamed Energy Propulsion, Vol. 997, pp. 367-378.

Yisheng, R., 2013, “Drag reduction research in supersonic flow with opposing jet”, Acta Astronautica, Vol. 91, pp. 1-7.

7. RESPONSIBILITY NOTICE